# α-Bungarotoxin-Sensitive Hippocampal Nicotinic Receptor Channel Has a High Calcium Permeability

Newton G. Castro and Edson X. Albuquerque

Department of Pharmacology and Experimental Therapeutics, University of Maryland School of Medicine, Baltimore, Maryland 21201-1559 USA, and Laboratório de Farmacologia Molecular II, Instituto de Biofísica Carlos Chagas Filho, Universidade Federal do Rio de Janeiro, Rio de Janeiro, RJ, Brazil

ABSTRACT The hippocampal nicotinic acetylcholine receptor (nAChR) is a newly identified ligand-gated ion channel that is blocked by the snake toxin α-bungarotoxin (α-BGT) and that probably contains the α7 nAChR subunit in its structure. Here its ion selectivity was characterized and compared with that of the *N*-methyl-D-aspartate (NMDA) receptor channel. The reversal potentials ($V_R$) of acetylcholine- and NMDA-activated whole-cell currents were determined under various ionic conditions. Using ion activities and a Goldman-Hodgkin-Katz equation for $V_R$ shifts in the presence of $Ca^{2+}$, permeability ratios were calculated. For the α-BGT-sensitive nAChR, $P_{Na}/P_{Cs}$ was close to 1 and $Cl^-$ did not contribute to the currents. Changing the $[Ca^{2+}]_0$ from 1 to 10 mM, the $V_R$s of the nAChR and NMDA currents were shifted by +5.6 ± 0.4 and +8.3 ± 0.4 mV, respectively, and the nAChR current decay was accelerated. These shifts yielded $P_{Ca}/P_{Cs}$s of 6.1 ± 0.5 for the nAChR channel and 10.3 ± 0.7 for the NMDA channel. Thus, the neuronal α-BGT-sensitive nAChR is a cation channel considerably selective to $Ca^{2+}$ and may mediate a fast rise in intracellular $Ca^{2+}$ that would increase in magnitude with membrane hyperpolarization.

## INTRODUCTION

Nicotinic acetylcholine receptors (nAChRs) are widely distributed in the vertebrate brain, yet their physiological function in situ is poorly understood (Sargent, 1993). These receptor macromolecules constitute a family of ligand-gated ion channels, presumably similar in structure to the muscle endplate nAChR channel, but having fundamentally diverse pharmacological and functional properties. The neuronal nAChRs are built from combinations of two types of integral protein subunits, termed α (containing a pair of cysteines that form part of the agonist-binding domain) and β. Whole-cell patch-clamp recordings in cultured rat hippocampal neurons have permitted the identification of three types of nAChR currents, which differ in their $EC_{50}$ of acetylcholine (ACh), their blockade by specific antagonists, and their likely subunit composition (Alkondon and Albuquerque, 1991, 1993). Most neurons in that preparation express a type of nAChR that, when activated by a saturating agonist concentration (1–3 mM for ACh), gives rise to a whole-cell current that activates and inactivates (desensitizes) fast and completely. This nAChR current is unique in being selectively blocked by the snake toxin α-bungarotoxin (α-BGT) (Alkondon and Albuquerque, 1991, 1993; Zorumski et al., 1992) and by picomolar concentrations of methyllycaconitine (MLA, Alkondon et al., 1992; Alkondon and Albuquerque, 1993). Because of its functional similarities with the recombinant, homomeric α7 nAChR expressed transiently in *Xenopus* oocytes (Schoepfer et al., 1990; Couturier et al., 1990; Séguéla et al., 1993), it is presumed that the α-BGT-sensitive hippocampal receptor is composed of α7 subunits (Alkondon and Albuquerque, 1993; Alkondon et al., 1994; Zorumski et al., 1992). Accordingly, the α7 mRNA is expressed at high density in hippocampal neurons both in situ (Schoepfer et al., 1990; Couturier et al., 1990; Séguéla et al., 1993) and in dissociated culture (Alkondon et al., 1994). At the unitary-current level, the hippocampal α-BGT-sensitive nAChR channel can be distinguished by its brief lifetime and high conductance, and by its inactivation in less than 1 ms (Castro and Albuquerque, 1993). This nAChR has also been identified in acutely dissociated neurons from the CA1 hippocampal field of 4- to 25-day-old rats (Ishihara et al., 1994), ascertaining its occurrence in vivo.

To characterize further the functional properties of this novel ACh-gated channel, we have investigated its ion selectivity. For this purpose, we applied the Goldman-Hodgkin-Katz (GHK) constant-field model (Goldman, 1943; Hodgkin and Katz, 1949), obtaining ionic permeability ratios from current reversal potentials ($V_R$s) measured in cultured rat hippocampal neurons. The α-BGT-sensitive ACh currents were functionally and pharmacologically isolated from other cholinergic responses that might have been present. To facilitate comparison of results from different studies, permeability measurements were performed in parallel on nAChR and glutamate receptor channels. Our results demonstrate that the most prevalent hippocampal nAChR has the highest $Ca^{2+}$ permeability among the native nAChRs described to date. Because the recombinant α7 nAChR was recently shown to have a very high relative permeability to $Ca^{2+}$ (Bertrand et al., 1993; Sands et al., 1993; Séguéla et al., 1993), the present data are consistent with the channel containing α7 subunits. As in the case of the NMDA subtype of glutamate receptor, the $Ca^{2+}$ permeability may be the key to

*Received for publication 16 September 1994 and in final form 3 November 1994.*

Address reprint requests to Dr. Edson X. Albuquerque, Department of Pharmacology and Experimental Therapeutics, University of Maryland School of Medicine, 655 West Baltimore Street, Baltimore, MD 21201-1559. Tel.: 410-706-7330; Fax: 410-706-3991; E-mail: ealbuquer@umabnet.ab.umd.edu.

© 1995 by the Biophysical Society

0006-3495/95/02/516/09 $2.00

understanding the role of the α-BGT-sensitive nAChRs in the brain. Some of the data appeared previously in abstract form (Castro et al., 1993; Castro and Albuquerque, 1994).

## MATERIALS AND METHODS

### Cell culture

Hippocampal neuron cultures were prepared as previously described (Alkondon and Albuquerque, 1993). Briefly, 17- to 18-day-old Sprague-Dawley rat fetuses were sacrificed under $CO_2$ narcosis, the hippocampi were dissected, and hippocampal tissue was mechanically dissociated after trypsinization. The neurons were plated on 35-mm collagen-coated culture dishes and were maintained in a modified Eagle's medium supplemented with l-glutamine and 10% horse serum. One week after plating, glial cell proliferation was inhibited with 2-fluoro-5′-deoxyuridine. To avoid possible age-dependent variations of the measured parameters, and to increase the probability of finding large ACh currents (Alkondon and Albuquerque, 1991), the recordings were performed only between 20 and 29 days after plating the cells.

### Recordings

Whole-cell patch-clamp recordings (Hamill et al., 1981) were performed either with a List EPC-7 (List-electronic, Darmstadt, Germany) or an Axopatch 200A amplifier (Axon Instruments, Foster City, CA) at 22–23°C. The receptor agonists were applied via a thin-glass U-tube device (Alkondon and Albuquerque, 1993), and the bath and agonist solutions had the same ionic composition at all times. A disk made of cured Sylgard with a long, rectangular hole cut out was sealed onto the culture dish, creating a 0.4 ml recording chamber. The external (bath) solutions were applied to one end of the chamber at a rate of 0.8–1 ml/min and were removed both by the U-tube and by siphons at the opposite end. External solutions were exchanged by rapidly running ~4 ml of the new solution. The reference electrode was an Ag/AgCl pellet connected to the bath via a coarse-tip, 3 M-KCl agar bridge placed downstream in the chamber. The microelectrode offset was adjusted to zero before sealing and never changed by more than 0.5 mV during an experiment. Patch electrodes were pulled from borosilicate glass capillaries and heat-polished, yielding resistances of 2–3 MΩ. The maximum access resistance was 14 MΩ, and it was not compensated for. After the cell membrane was broken, the cytoplasm was allowed to dialyze with the pipet solution for 4 min before recording the first response. The recordings were started in the $Na^+$-based standard external solution (see below), and the solutions were subsequently switched in no particular order.

### Solutions

Reversal potential determinations were done with a fixed, Cs-based intracellular solution and different extracellular solutions (Table 1). The main internal solution ("ATP-R internal solution") included a high-energy phosphate regenerating system (MacDonald et al., 1989), which was found to minimize the run-down of α-BGT-sensitive nAChR currents (Alkondon et al., 1994). Concentrated aqueous solutions of the three ingredients, adenosine 5′-triphosphate (ATP), phosphocreatine (PC), and creatine phosphokinase (CPK), were kept frozen in small aliquots, and were added just before the experiment to an appropriately concentrated internal solution containing the remaining components. The final ATP-R internal solution was kept on ice during the experiments and had the following composition (in mM): CsCl 60, CsF 60, CsOH 38.5, $MgCl_2$ 5, EGTA 10, HEPES 10, ATP 5, PC 20, Tris 52.5, and CPK 50 units/ml (pH 7.3, 340 mOsm/kg). Another standard internal solution, without the ATP system, was used in a set of preliminary experiments. The cells were patch-clamped in a Na-based external solution, which was (in mM): NaCl 165, KCl 5, $CaCl_2$ 2, $MgCl_2$ 2, HEPES 5, D-glucose 10, NaOH ~2 (pH 7.3, 340 mOsm/kg). The junction potential between the $Na^+$-based standard external solution and both the standard and ATP-R internal solution was 7 mV. This value was subtracted from all of the membrane potentials. The main test external solutions included both $Cl^-$ and methanesulfonate salts, to bring the $Cl^-$ equilibrium potential close to 0 mV. The external solutions containing 150 mM $Cs^+$ or $Na^+$ also had *N*-methyl-D-glucamine (NMG) and HCl (to bring the osmolarity to 340 mOsm/kg and the pH to 7.3), plus 10 mM D-glucose and 10 mM HEPES. All salts used were of the highest grade. The following antagonists were included in all the test solutions to ensure that only the α-BGT-sensitive nAChR contributed to the recorded currents (in μM): tetrodotoxin 0.3, atropine sulphate 1, DL-2-amino-5-phosphonovaleric acid 50 (excluded when testing NMDA currents), 6-cyano-7-nitroquinoxaline-2,3-dione (CNQX) 10, picrotoxin 50, and dihydro-β-erythroidine hydrobromide (DHβE) 0.1. The receptor agonists were acetylcholine chloride (ACh) 1 mM, NMDA 50 μM plus glycine 10 μM, quisqualic acid (quisqualate) 50 μM, and γ-amino-*n*-butyric acid (GABA) 10 μM. All drugs were from Sigma Chemical Co. (St. Louis, MO), except CNQX, which was from Research Biochemicals International (Natick, MA), and DHβE, which was a gift from Merck, Sharp & Dohme (St. Louis, MO).

### Analysis

The drug-induced whole-cell currents were digitized, stored, and measured using a personal computer operated with pCLAMP software (Axon Instruments). During acquisition, the currents were filtered at 500 Hz (analog, 8-pole Bessel) and sampled at 1 kHz. The slow NMDA currents were further digitally filtered at 100 Hz. For the peak current versus voltage (*I-V*) relationships, the holding potential was changed in 5- or 10-mV increments, driven by the computer. The membrane potentials were corrected for the small (2.5 mV maximum) voltage drop at the command input of the patch-clamp. The data points were plotted and fitted by a third-degree polynomial using SigmaPlot (Jandel Scientific, Corte Madera, CA), and the reversal potential ($V_R$) was determined as the relevant root of the polynomial. Only experiments in which the $V_R$ was bracketed by two or more data points on each side were included in the analysis. In most neurons, the *I-V* protocols

**TABLE 1 Ionic composition of the test solutions**

| | $Na^+$* | $K^+$ | $Cs^+$ | $NMG^+$ | $Ca^{2+}$ | $Mg^{2+}$ | $Cl^-$ | $CH_3SO_3^-$ | $F^-$ |
|---|---|---|---|---|---|---|---|---|---|
| External | | | | | | | | | |
| $Na^+$-based standard | 167 | 5 | | | 2 | 2 | 178 | | |
| $Na^+$-based $CH_3SO_3^-$ | 167 | 5 | | | 2 | 2 | 13 | 165 | |
| $Na^+$-based, 1 mM $Ca^{2+}$ | 150 (111) | | | 26 | 1 (0.28) | | 73 | 100 | |
| $Cs^+$-based, 1 mM $Ca^{2+}$ | | | 150 (105) | 35 | 1 (0.27) | | 83 | 100 | |
| $Cs^+$-based, 10 mM $Ca^{2+}$ | | | 150 (104) | 20 | 10 (2.74) | | 86 | 100 | |
| Internal | | | | | | | | | |
| Standard | | | 186 | | | | 82 | | 80 |
| ATP-R | | | 159 (105) | | | 5 | 70 | | 60 |

* Concentration in mM.

The values in parentheses to the right of the concentrations are the ion activities used in the calculations. The activity coefficients for $Na^+$ and $Cs^+$ were interpolated from Table 11, Appendix 8.10 of Robinson and Stokes (1970). Those for $Ca^{2+}$ were from Table I of Butler (1968), which applies to NaCl-$CaCl_2$ mixtures, and were squared according to Guggenheim's convention. The values were looked up in the tables using the calculated ionic strength of the test solutions.

were run twice or more in each ionic medium. The standard deviation of the $V_R$ among runs was usually under 0.5 mV, with a maximum of 1.2 mV. The mean values from individual neurons were used to calculate the grand mean ± SEM reported for each ionic condition. One expression derived from the "extended" GHK equation (Lewis, 1979) was used to calculate relative ion permeabilities with respect to $Cs^+$ ($P_X/P_{Cs}$), in the presence of $Ca^{2+}$. The expression gives permeability ratios from pairs of $V_R$ measurements ($V_{R1}$ and $V_{R2}$) obtained in two different extracellular solutions. Starting from the equation in the form given by Lewis (1979), considering only $Cs^+$ and $Ca^{2+}$, and letting $\Delta V_R = V_{R2} - V_{R1}$, one obtains

$$\Delta V_R = \frac{RT}{F} \ln \frac{Cs_{o2} + P_{Ca}/P_{Cs} Ca_{o2}(1 + e^{V_{R2}F/RT})^{-1}}{Cs_{o1} + 4P_{Ca}/P_{Cs} Ca_{o1}(1 + e^{V_{R1}F/RT})^{-1}}, \quad (1)$$

where $Cs_{o1}$, $Ca_{o1}$, $Cs_{o2}$, and $Ca_{o2}$ are the bulk ion activities outside the cell, and $R$, $T$, and $F$ have their usual meanings. At room temperature, $RT/F$ was taken to be 25.5 mV. This expression can be solved for $P_{Ca}/P_{Cs}$, yielding

$$\frac{P_{Ca}}{P_{Cs}} = \frac{Cs_{o2} - Cs_{o1} e^{\Delta V_R F/RT}}{4Ca_{o1} e^{\Delta V_R F/RT}(1 + e^{V_{R1}F/RT})^{-1} - 4Ca_{o2}(1 + e^{V_{R2}F/RT})^{-1}}. \quad (2)$$

When substituting extracellular $Cs^+$ by $Na^+$, an analogous expression can be derived,

$$\frac{P_{Na}}{P_{Cs}} = \frac{Cs_{o1} e^{\Delta V_R F/RT}}{Na_{o2}} + \frac{4P_{Ca}/P_{Cs}}{Na_{o2}} [Ca_{o1} e^{\Delta V_R F/RT}(1 + e^{V_{R1}F/RT})^{-1} - Ca_{o2}(1 + e^{V_{R2}F/RT})^{-1}]. \quad (3)$$

In addition to being independent of the intracellular medium, these expressions have the additional advantage of minimizing the influence of systematic errors in the measurements of the absolute $V_R$. Incomplete space clamping, for instance, could cause such errors in the absolute $V_R$ estimates, although not affecting $\Delta V_R$ to the same extent. The analysis of parameter sensitivities in our experimental conditions showed that for measured shifts in the range of 5–10 mV, an error of up to ±5 mV in $V_{R1}$ (and so in $V_{R2}$) changes the calculated $P_{Ca}/P_{Cs}$ by a maximum of ±13%.

## RESULTS

### Characteristics of the α-BGT-sensitive ACh responses

The cultured hippocampal neurons sampled in this study showed the same types of ACh currents described previously (Alkondon and Albuquerque, 1991, 1993; Alkondon et al., 1992; Castro and Albuquerque, 1993). Over 80% of the neurons responded to ACh (1 mM) with currents greater than 50 pA. Currents corresponding to the α-BGT-sensitive, low-affinity, fast-desensitizing nAChR (α7-type; Alkondon and Albuquerque, 1993) were by far the most prevalent (about 83% of the neurons sampled), but currents corresponding to the DHβE-sensitive, high affinity, slowly desensitizing nAChR (α4β2-type), as well as a hybrid variant, were also observed. Only the neurons showing an apparently pure, fast-desensitizing ACh-induced current were included in the permeation study. Additionally, all of the $V_R$ measurements used in the permeability-ratio calculations were obtained with DHβE (0.1 μM) in the bath. At this concentration, DHβE would have blocked the current evoked by activation of the α4β2-type nAChR that, in some neurons, is expressed together with the α7-type nAChR (Alkondon and Albuquerque, 1993; Castro and Albuquerque, 1993).

### Preliminary assessment of the $Ca^{2+}$ permeability

In these experiments, the standard internal solution (Table 1) was used and, as previously described (Alkondon and Albuquerque, 1993), a marked rundown of the ACh response was apparent. This, however, did not affect the $V_R$ determinations, which were reproducible at different times during the experiments and insensitive to whether the membrane potential was stepped in the positive or negative direction. Because the rundown appeared to be mostly agonist-independent, its distorting effect on the current-voltage ($I$-$V$) relationship could be minimized by reducing the interval between ACh applications. An inter-pulse interval of 8 s was sufficient to allow for a nearly complete recovery of the sensitivity of the nAChR. This duration interval was selected to study ACh-evoked currents at various holding potentials, whereas longer intervals were used to examine NMDA or quisqualate currents.

The $V_R$s of ACh, NMDA, and quisqualate currents were measured in the $Na^+$-based standard external solution, which had 2 mM $Ca^{2+}$, and in a similar solution containing 10 mM $Ca^{2+}$ (Fig. 1). Under all experimental conditions, the ACh $I$-$V$ relationship showed some degree of inward rectification,

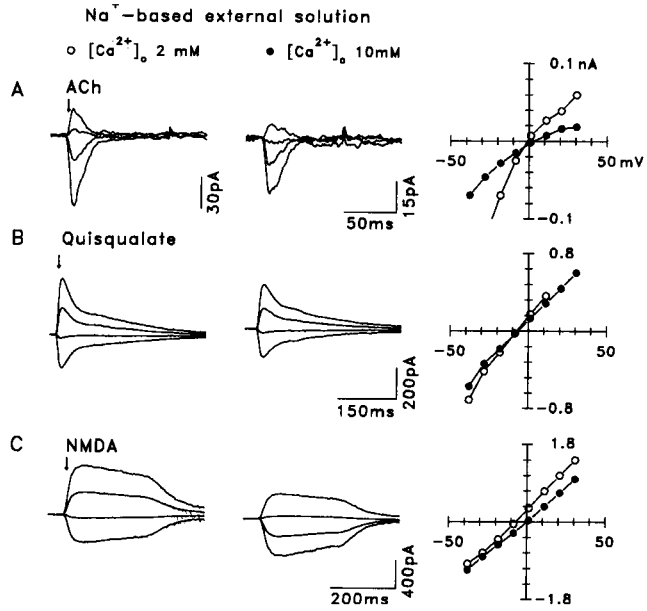


FIGURE 1 Reversal potential measurements made with the standard internal solution and either the $Na^+$-based standard external solution (2 mM $Ca^{2+}$, ○) or the $Na^+$-based solution containing 10 mM $Ca^{2+}$ (●). Each panel shows current traces obtained at +11, +1, −8, and −18 mV, and the corresponding $I$-$V$ plot on the right. (*A*) The $V_R$ of currents activated by ACh (1 mM) depends on external $Ca^{2+}$. The $V_R$ was −0.7 mV in 2 mM, and 3.1 mV in 10 mM $Ca^{2+}$. (*B*) In the same neuron, the quisqualate-activated current $V_R$ is more negative and less $Ca^{2+}$-dependent than the ACh current $V_R$. The $V_R$ was −7.4 mV in 2 mM and −7.3 mV in 10 mM $Ca^{2+}$. Although ACh responses showed a marked rundown during the 20-min interval between the two $V_R$ measurements (see *A*), responses to quisqualate (50 μM) were little affected. (*C*) The $V_R$s in 2 mM and 10 mM $Ca^{2+}$ were −7.1 and −0.3 mV, respectively, whereas in the same neuron (not shown) the ACh $V_R$s were −1.8 and 2.0 mV, respectively, indicating that the $V_R$ of currents activated by NMDA (50 μM, plus 10 μM glycine) is more $Ca^{2+}$-dependent than that of ACh currents.

characterized by a smaller conductance between -10 and 30 mV. Using the $Na^+$-based external solution, which had 2 mM $Ca^{2+}$, the ACh current $V_R$ was found to be -1.9 ± 0.8 mV. When the concentration of $Ca^{2+}$ was increased to 10 mM, the $V_R$ of the ACh currents became more positive by 3.7 ± 0.1 mV ($n$ = 3). Fig. 1 *B* shows that, in contrast to the ACh current $V_R$, the $V_R$ of the quisqualate current on the same neuron was little affected by a fivefold increase in $Ca^{2+}$ concentration. The $V_R$ of the quisqualate current only became totally independent of $Ca^{2+}$ when the concentration of quisqualate was under 5 μM, and that of APV was above 100 μM, probably because otherwise NMDA channels were also being activated (Iino et al., 1990). Using the $Na^+$-based external solution, the NMDA current $V_R$ was −6.1 ± 0.7 mV. This value was shifted to 5.5 ± 0.5 mV ($n$ = 8) upon changing the external $Ca^{2+}$ concentration from 2 to 10 mM. These results suggested that a significant fraction of both the ACh and NMDA currents was carried by $Ca^{2+}$.

Upon increasing the $Ca^{2+}$ concentration, not only $Ca^{2+}$, but also $Cl^-$ was present in higher concentration. Thus, if $Cl^-$ contributed to the ACh currents, the $V_R$ shift would have underestimated the $Ca^{2+}$ permeability of the nAChR channel relative to that of the NMDA channel, which is selective for cations. To examine this possibility using the standard external solution, the equilibrium potential for $Cl^-$ ($E_{Cl}$) was estimated by measuring the $V_R$ of GABA currents. The value obtained was −19.4 ± 0.7 mV ($n$ = 3). That the ACh current $V_R$ was about 18 mV more positive than $E_{Cl}$, and also more positive than the quisqualate current $V_R$, suggested that $Cl^-$ contributed little, if at all, to the ACh currents. This was confirmed directly in the experiments described next.

## Reversal potentials shifts

In this set of experiments, the ACh current rundown was reduced by using the ATP-R internal solution in the recording pipette. The ACh current $V_R$ in ATP-R internal solution and in standard external solution was 3.9 ± 0.3 mV ($n$ = 7). This value was more positive than that obtained in standard internal solution, as was expected because of the lower concentration of $Cs^+$ in the ATP-R internal solution. The $Cl^-$ permeability of the ACh channel was assessed by substituting the larger anion methanesulfonate for $Cl^-$. If $Cl^-$ were permeant, one would expect a positive shift of the $V_R$. In contrast, the $V_R$ became more negative by 4.7 ± 0.5 mV ($n$ = 3, see Fig. 2). One possible explanation for this shift would have been a smaller cation activity in methanesulfonate-based external solution than in the standard external solution. Consistent with that, the amplitude of the ACh current was reduced in methanesulfonate-based external solution and partially recovered after changing back to $Na^+$-based standard external solution.

The $Ca^{2+}$-dependent changes in $V_R$ were tested with $Cs^+$ as the main cation on both sides of the membrane, and with extracellular $Ca^{2+}$ concentrations bracketing the physiological level. After changing the $Na^+$-based standard external solution to either one of the $Cs^+$-based external solutions (see

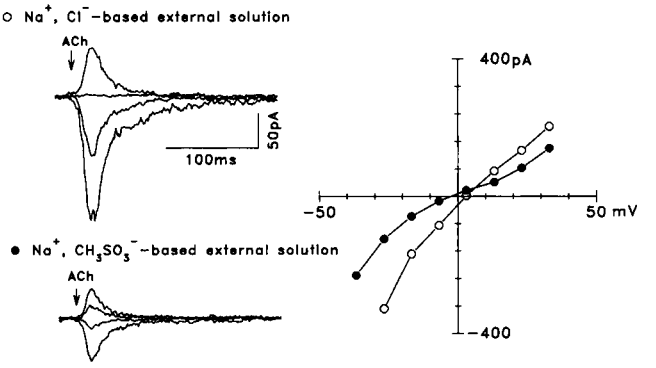


FIGURE 2 Chloride did not contribute significantly to the ACh currents: substituting external $Cl^-$ by methanesulfonate caused a negative $V_R$ shift. The *I-V* relationships were obtained with the ATP-R internal solution and either the $Na^+$-based standard external solution (○) or the methanesulfonate-based external solution (●). The $V_R$s were 3.3 mV in $Na^+$-based standard external solution, and −1.9 mV in methanesulfonate-based external solution.

Table 1), the peak ACh current was markedly reduced, in a way similar to that observed in adrenal chromaffin cells (Hirano et al., 1987), PC12 cells (Neuhaus and Cachelin, 1990), and in rat sympathetic neurons (Mathie et al., 1991). This reduction was evident in the first ACh response in a $Cs^+$-based solution, progressed slowly despite the ATP-R internal solution (see Alkondon et al., 1994), and was only partially reversible upon returning to the $Na^+$-based standard external solution.

Fig. 3 shows the results of the $V_R$ determinations in the $Cs^+$-based external solutions. Using $Cs^+$-based external solution containing $Ca^{2+}$ (1 mM), the $V_R$ of ACh currents was −3.0 ± 0.4 mV, whereas that of NMDA currents was −2.7 ± 0.3 mV. For both current types, the $V_R$ was significantly more positive when $Ca^{2+}$ concentration was increased to 10 mM, as would be expected if $Ca^{2+}$ were a major charge carrier. The $V_R$ of the ACh current became 2.6 ± 0.5 mV (shifting by 5.6 ± 0.4 mV, $n$ = 5), whereas that of the NMDA current became 5.6 ± 0.3 mV (shifting by 8.3 ± 0.4 mV, $n$ = 8). On the basis of the $V_R$ shifts, the α-BGT-sensitive, neuronal nAChR channel was highly permeable to $Ca^{2+}$, but less so than the NMDA channel.

The $V_R$s of both ACh and NMDA currents in $Cs^+$-based external solution containing 1 mM $Ca^{2+}$ were more negative than the calculated $E_{Cs}$ which, based upon the ion activities (in Table 1), should be close to 0 mV. Because the $Cs^+$ ion activity could not be measured experimentally, and published data for the methanesulfonate salts were not available, the activities shown in Table 1 were estimated as if all of the anion was $Cl^-$. However, the result with the methanesulfonate-based external solution suggested that at the concentrations used, methanesulfonate salts of the alkali metals may have yielded lower cation activities than the corresponding chlorides. If this was the case, the $V_R$ of the quisqualate current, which is carried by monovalent cations, should have been more negative than that of the ACh and NMDA currents, reflecting the actual value of $E_{Cs}$. Indeed,

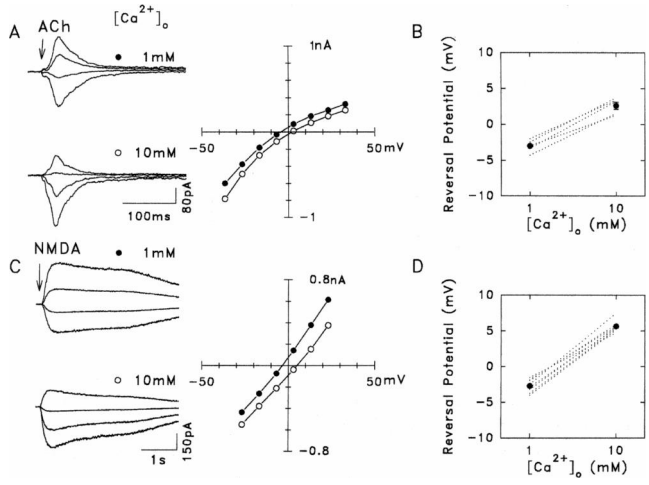


FIGURE 3 $V_R$ measurements made with the ATP-R internal solution and either the $Cs^+$-based external solution containing 1 mM $Ca^{2+}$ (●) or the $Cs^+$-based external solution containing 10 mM $Ca^{2+}$ (○). The curves in the *I-V* plots are the third-degree polynomials used to interpolate the $V_R$. (*A*) Sample experiment in which the ACh current $V_R$ was −4.4 mV in $Cs^+$-based external solution containing 1 mM $Ca^{2+}$, and 1.9 mV in $Cs^+$-based external solution containing 10 mM $Ca^{2+}$. The currents in $Cs^+$-based external solution containing 1 mM $Ca^{2+}$ were recorded about 15 min after those in $Cs^+$-based external solution containing 10 mM $Ca^{2+}$, which may explain the small difference in amplitude due to rundown. (*B*) ACh $V_R$ data from five neurons. The results from each neuron are represented by a straight line; the mean and SEM of the $V_R$ in each solution is depicted by the filled circle and its error bars. (*C*) Sample experiment in which the NMDA current $V_R$ was −2.9 mV in $Cs^+$-based external solution containing 1 mM $Ca^{2+}$, and 5.4 mV in $Cs^+$-based external solution containing 10 mM $Ca^{2+}$. (*D*) NMDA $V_R$ data from eight neurons, showing larger shifts than that seen with ACh currents in *B*. The small vertical error bars refer to SEM.

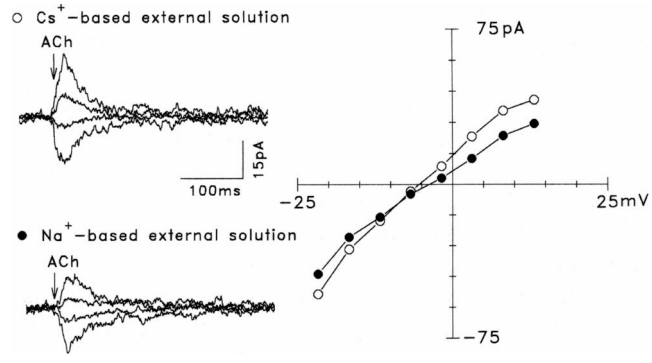


FIGURE 4 Sodium-cesium relative permeability, evaluated by total substitution in the external solution. ACh current $V_R$ measurements were made with the ATP-R internal solution and either the $Cs^+$-based external solution containing 1 mM $Ca^{2+}$ (○) or the Na-based external solution containing 1 mM $Ca^{2+}$ (●). In the two runs shown, the $V_R$s were −5.3 mV in $Cs^+$-based external solution containing 1 mM $Ca^{2+}$, and −3.8 mV in Na-based external solution containing 1 mM $Ca^{2+}$. The shift could be accounted for by the difference in ion activity of the two cations (see Table 1). Current traces shown were recorded at +3, −2, −7, and −12 mV.

the $V_R$ of the currents activated by quisqualate (1 μM, in the presence of APV 250 μM) was −5.6 ± 0.7 mV in the $Cs^+$-based external solution with 1 mM $Ca^{2+}$, and was not detectably different in $Cs^+$-based external solution containing 10 mM $Ca^{2+}$. Thus, it can be assumed that $E_{Cs}$ was close to −5.6 mV and that, in the methanesulfonate-containing solutions, the cation activities were smaller than stated in Table 1. The $Na^+$ permeability of the nAChR was estimated from the $V_R$ shifts observed after total substitution of $Cs^+$ by $Na^+$ in the external solution (Fig. 4). In the $Na^+$-based solution with 1 mM $Ca^{2+}$, the $V_R$ became 1.6 mV more positive than in $Cs^+$-based external solution containing 1 mM $Ca^{2+}$ (8 $V_R$ determinations from 1 neuron).

## Analysis of the $V_R$ findings using GHK equations

The GHK equations depicted under Materials and Methods were used to estimate the permeability ratios from the $V_R$ data. To apply the GHK model to our experimental conditions, it was assumed that only $Cs^+$, $Na^+$, and $Ca^{2+}$ contributed to the currents. Substitution in Eq. 1 of the pairs of $V_R$s obtained in the $Cs^+$-based external solution containing either 1 mM $Ca^{2+}$ ($V_{R1}$) and 10 mM ($V_{R2}$) solutions yielded an average $P_{Ca}/P_{Cs}$ of 6.1 ± 0.5 for the ACh channel, and of 10.3 ± 0.7 for the NMDA channel. Equation 3 was used to estimate $P_{Na}/P_{Cs}$ from the $V_R$ shifts in the presence of $Ca^{2+}$ 1 mM. Because the ACh channels showed a high $Ca^{2+}$ permeability, ignoring the contribution of $Ca^{2+}$ would have produced erroneous results. The positive $V_R$ shift observed when switching from 150 mM $Cs^+$ to 150 mM $Na^+$ could be accounted for by the higher $Na^+$ ion activity, with the calculated $P_{Na}/P_{Cs}$ of the nAChR being close to 1.0.

The effect of putative surface potentials ($\Psi$) due to fixed charges in the vicinity of the channel was examined. Most cation channels contain negative charges near to the pore that seem to contribute to ion selectivity (Green and Andersen, 1991). The magnitude of the surface potential associated with these charges is reduced by their interaction with cations in the bath, particularly the divalent ones. The experiments were designed to minimize the differences in $\Psi$ among test solutions, e.g., NMG-Cl was used as an osmotic substitute to keep the ionic strength of the solutions fairly constant and similar to the physiological levels. However, depending upon the actual surface charge density ($\sigma$), a significant negative $\Psi$ could have remained in all solutions, contributing to the overall transmembrane potential. The magnitude of $\Psi$ in $Cs^+$-based external solution containing 1 or 10 mM $Ca^{2+}$ was calculated using Gouy-Chapman theory (see Lewis, 1979), assuming values of $\sigma$ ranging from 0.02 to 0.2 electronic charges per $nm^2$. $P_{Ca}/P_{Cs}$ was then obtained with Eq. 2, which was modified by substituting the membrane potential $V$ by $(V - \Psi)$, and the bulk ion activities $X_o$ by the surface activities $X_s$ (given by $X_s = X_o \exp(-z_X F\Psi/RT)$). Table 2 gives the relationship of $\sigma$ to the calculated $P_{Ca}/P_{Cs}$.

Besides $Cs^+$, $Na^+$, and $Ca^{2+}$, the other cations present at significant concentration were $NMG^+$ and $Tris^+$, which was probably about 86% ionized in the ATP-R internal solution. In an attempt to explain why the $V_R$s in $Cs^+$-based external solution containing 1 mM $Ca^{2+}$ were more negative than $E_{Cs}$ (Castro et al., 1993), the intracellular $Tris^+$ had initially been considered to be permeant. However, it has been recently

**TABLE 2 Effect of negative surface charges on the permeability ratios**

| | $\Psi$ (mV)‡ | | $P_{Ca}/P_{Cs}$ | |
|---|---|---|---|---|
| $\sigma$ ($e$/nm$^2$)* | $Cs^+$-based 1 mM $Ca^{2+}$ | $Cs^+$-based 10 mM $Ca^{2+}$ | ACh | NMDA |
| – | – | – | 6.1 | 10.3 |
| 0.02 | −3.6 | −4.4 | 5.5 | 9.5 |
| 0.05 | −9.3 | −10.1 | 5.1 | 8.7 |
| 0.10 | −18.6 | −19.2 | 4.5 | 7.9 |
| 0.20 | −35.3 | −35.3 | 3.9 | 6.9 |

* $\sigma$ refers to surface charge density.
‡ $\Psi$ refers to surface potential.

observed that $Tris^+$ does not permeate the NMDA channel (M. M. Zarei and J. A. Dani, personal communication), and the lowering of the extracellular cation activity by methanesulfonate was sufficient to account for the $V_R$ offsets of the ACh, NMDA, and quisqualate currents simultaneously. Even if $Tris^+$ was permeant, which remains to be tested, $P_{Ca}/P_{Cs}$ and $P_{Na}/P_{Cs}$ would not have been affected. The larger cation, $NMG^+$, does not contribute to either NMDA or quisqualate currents (Iino et al., 1990; Zarei and Dani, 1994), and is also unlikely to have contributed to the ACh currents. If $NMG^+$ was actually permeant in the nAChR, including it in the calculations would boost the estimated $P_{Ca}/P_{Cs}$. As an example, for a $P_{NMG}/P_{Cs}$ of 0.25, $P_{Ca}/P_{Cs}$ would be about 15% higher.

### Effect of $Ca^{2+}$ on the ACh current decay

The effect of extracellular $Ca^{2+}$ on the desensitization kinetics of the nAChR channel was also examined. The currents evoked by 0.5- or 1-s pulses of 1 mM ACh varied from cell to cell in amplitude and, to some extent, in kinetics. The 10–90% risetime ranged from 6.9 to 18.6 ms, averaging 13.2 ± 0.5 ms. The decays were usually fitted by two exponentials with 5–10 times differences in time constants. The fastest decay time constant (at −67 mV, using $Na^+$-based standard external solution) ranged from 9.1 to 59.7 ms and averaged 23.6 ± 2.1 ms. These kinetic parameters seemed to depend on the size and neurite distribution of the neurons. To avoid cell-to-cell variability, the responses under different $Ca^{2+}$ conditions were compared in the same neuron. As illustrated in Fig. 5, the ACh current decay was accelerated when extracellular $Ca^{2+}$ concentration was raised from 1 to 10 mM. This was true when comparing the inward currents, recorded at −67 or −37 mV, and also in the case of outward currents, recorded at +33 mV.

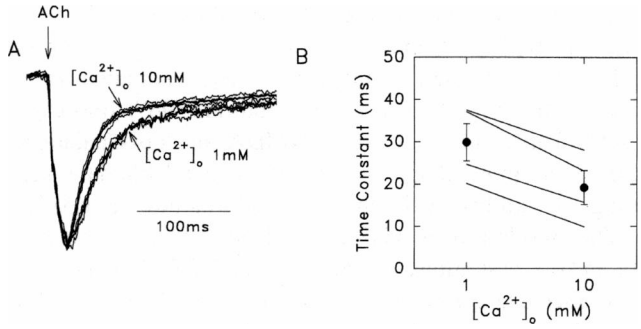


FIGURE 5 The ACh current decay became faster upon raising the external $Ca^{2+}$ concentration. (*A*) ACh currents recorded at −67 mV in $Cs^+$-based external solution containing 1 mM $Ca^{2+}$ and in $Cs^+$-based external solution containing 10 mM $Ca^{2+}$ from the same neuron. To emphasize the difference in the decay rates, three superimposed traces recorded in each $Ca^{2+}$ condition and their averages (*thick line*) are shown. The currents were scaled up to the same peak amplitude and aligned at the midpoint of the rising phase. (*B*) $Ca^{2+}$-dependent changes in the fast time constant of decay of the ACh current. The lines depict the changes observed in four neurons. The mean difference between the time constants in 1 and 10 mM $Ca^{2+}$ was 10.7 ± 1.1 ms, being significantly different from zero ($p < 0.01$, paired $t$ test). The ACh currents from all neurons showed a faster decay in $Cs^+$-based external solution containing 10 mM $Ca^{2+}$ than in $Cs^+$-based external solution containing 1 mM $Ca^{2+}$, whether at negative (−37 mV for the data shown) or at positive (+33 mV) membrane potentials.

## DISCUSSION

### Comparison with other $Ca^{2+}$ permeability data

The present results demonstrate that the main type of nAChR channel in hippocampal neurons is cationic and greatly favors $Ca^{2+}$ as a charge carrier. The GHK model was used to permit reliable comparisons with available experimental data gathered from various preparations. To support further these comparisons, the reversal potential determinations and the GHK analysis were performed in the same manner for ACh-, NMDA-, and quisqualate-gated currents. Several potential sources of error in the permeability ratio calculations were taken into account, including the uncertainty of the ion activities in the complex intracellular solutions and the contribution of $Ca^{2+}$ in the experiments with monovalent ions. Although direct tests of the presence of a surface potential on the ACh channel were not performed, the influence of this parameter on the calculated $P_{Ca}/P_{Cs}$ was addressed. The results depicted in Table 2 show that with increasing $\sigma$ and $\Psi$, the surface activities of the cations involved would increase; however, that of $Ca^{2+}$ would increase faster than that of $Cs^+$. Consequently, the observed $V_R$ shifts would be explained by smaller $P_{Ca}/P_{Cs}$. It can be noted that, if the ACh and NMDA channels had the same $\sigma$, the relationship between the two $P_{Ca}/P_{Cs}$ would remain close to 60%, despite the smaller absolute values.

Our estimate of $P_{Ca}/P_{Cs}$ for the NMDA receptor channel of 10.3 compares with the values of 10.6 (Mayer and Westbrook, 1987), 14.3 (Iino et al., 1990), and 12 (Zarei and Dani, 1994) obtained previously. The small discrepancy between the previous data and ours is, at least in part, due to the choice of $Ca^{2+}$ activity coefficients. For instance, although Mayer and Westbrook's coefficients were similar to ours ($\gamma_{++}$ of 0.29 to 0.28, for $Ca^{2+}$ 1 to 10 mM), Zarei and Dani used lower values, which tends to inflate $P_{Ca}/P_{Cs}$. Using their values, we would also obtain a $P_{Ca}/P_{Cs}$ of 12 from our NMDA data, whereas from the ACh data, $P_{Ca}/P_{Cs}$ would be 7. Ascher and Nowak (1988) calculated $P_{Ca}/P_{Cs}$ (assumed equal to $P_{Ca}/P_{Na}$) based upon single-channel NMDA currents.

Converting ion concentrations to activities, their $V_R$ values yield a $P_{Ca}/P_{Cs}$ of about 13. In contrast, $P_{Ca}/P_{Cs}$ for the quisqualate-activated channel has been estimated to be smaller than 0.4 (Mayer and Westbrook, 1987; Iino et al., 1990). Thus, our results with NMDA and quisqualate receptors are in good agreement with the available data, verifying the validity of the method used to study the nAChR.

The muscle-type nAChR channels have a $P_{Ca}/P_{Cs}$ between 0.1 and 0.2, assuming a $P_{Cs}/P_{Na}$ of 1.4 and including the effect of surface charges (Lewis, 1979; Adams et al., 1980). More recently, it has been shown that α-BGT-insensitive neuronal nAChRs in several preparations are more permeable to $Ca^{2+}$ than is the muscle nAChR. The following $P_{Ca}/P_{Na}$ have been reported: in rat parasympathetic ganglia, 0.93 (Fieber and Adams, 1991) and 0.65 (Adams and Nutter, 1992), and in pheochromocytoma (PC12) cells, 2.5 (Sands and Barish, 1991). In adrenal chromaffin cells, $P_{Ca}/P_{Cs}$ has been calculated to be 1.5 (Vernino et al., 1992) and, using a quantitative fluorimetric method, the fraction of the nAChR current contributed by $Ca^{2+}$ has been found to be only 2.5% at −70 mV (Zhou and Neher, 1993). When comparing with the present results, it can be concluded that the predominant α-BGT-sensitive nAChR in hippocampal neurons has the highest selectivity for $Ca^{2+}$ among the native nAChRs.

The recombinant nAChR channel composed of α7 subunits and transiently expressed in *Xenopus* oocytes is also highly permeable to $Ca^{2+}$: increasing external $Ca^{2+}$ concentration from 1 to 10 mM caused the ACh current $V_R$ to shift by 29 mV in the positive direction (Séguéla et al., 1993). However, in the oocyte the ACh current triggers secondary endogenous $Ca^{2+}$-activated $Cl^-$ currents, which may have contributed to that $V_R$ shift. In another study of the α7 channel, the contamination by $Cl^-$ currents was minimized by using $Ba^{2+}$ outside, instead of $Ca^{2+}$, and by loading the oocytes with a fast $Ca^{2+}$ chelator (Sands et al., 1993). Under those conditions a high $P_{Ba}/P_{Na}$ of 16.6 was obtained (with $\sigma = 0.26$ $e/nm^2$), allowing one to infer that the $Ca^{2+}$ permeability of the α7 homomeric nAChR channel is indeed the highest among the recombinant nAChRs studied. Thus, high $Ca^{2+}$ permeability is yet another common property of the α-BGT-sensitive nAChR in the rat hippocampus and the recombinant α7 homomer. The present data support the proposal that the native hippocampal nAChR contains α7 subunits.

## Receptor modulation by $Ca^{2+}$

The rate of decay of the α-BGT-sensitive currents in the presence of ACh was $Ca^{2+}$ dependent, similar to what occurs in other preparations. Calcium modulates the rate of nicotinic current decay in muscles in at least two ways. When cholinesterase activity is present, increasing the extracellular $Ca^{2+}$ slows down the decay of endogenous endplate currents (spontaneous miniatures or nerve-evoked). This has been attributed to the net hyperpolarization of the membrane resulting from the binding and/or screening of negative surface charges by $Ca^{2+}$. The lengthening of the decay would then reflect the voltage-dependent increase in channel open time, which is the main determinant of the decay of endogenous currents. On the other hand, the current decay observed during sustained application of nicotinic agonists in anticholinesterase-treated endplates or in nAChR-expressing cell lines reflects receptor desensitization, and it is accelerated by increasing extracellular $Ca^{2+}$ concentration (reviewed in Ochoa et al., 1989). The site (or sites) of action of $Ca^{2+}$ is intracellular, and other divalent ions are much less effective. The mechanism may involve direct binding of $Ca^{2+}$ to the channel protein, or $Ca^{2+}$-triggered enzymatic modification of the channel, either leading to the stabilization of the desensitized state. Assuming that the ACh whole-cell currents in the hippocampal neurons passed exclusively through the 73-pS channel (Castro and Albuquerque, 1993), $Ca^{2+}$ probably affected the decay phase of the currents by modulating the desensitization rate rather than the channel open time. The latter is too short (~0.1 ms) to account for the observed decay time constants. In situ, desensitization of this receptor in addition to agonist removal is probably fast enough to be important in the termination of the response. The acceleration of desensitization may be a feedback mechanism limiting $Ca^{2+}$ entry through the channel, and it could also be promoted through other pathways that raise intracellular $Ca^{2+}$.

Calcium was recently shown to potentiate the response of α-BGT-insensitive neuronal nAChRs, including those natively expressed in chromaffin cells and in neurons from the medial habenula, and several recombinant ones expressed in *Xenopus* oocytes (Vernino et al., 1992; Mulle et al., 1992b). The potentiation depends on the concentrations of both $Ca^{2+}$ and the nicotinic agonist and appears to be mediated through an extracellular site. Using the various experimental solutions (Table 1), the ACh currents in the hippocampal neurons were not augmented by increasing extracellular $Ca^{2+}$. Because the $Ca^{2+}$-dependent potentiation can be overridden by increasing the agonist concentration, this effect may have been masked by the high concentration of ACh used here (1 mM). Alternatively, this type of modulation may be intrinsically lacking in the case of the α-BGT-sensitive nAChR. Consistent with that possibility, the α7-based recombinant nAChR does not show a positive modulation by external $Ba^{2+}$ (Sands et al., 1993).

## Implications to function in situ

The present permeability data indicate that the α-BGT-sensitive nAChR can mediate $Ca^{2+}$ entry into hippocampal neurons. This was confirmed directly in $Ca^{2+}$-imaging experiments done in the same preparation, where this nAChR triggered a fast, transient rise in the intracellular $Ca^{2+}$ concentration that was blocked by methyllycaconitine (1 nM; N. G. Castro, W. G. Wier, and E. X. Albuquerque, unpublished data). A similar nAChR is also expressed in chick ciliary ganglia, as shown by $Ca^{2+}$ fluorimetry (Vijayaraghavan et al., 1992) and current recording (Zhang et al., 1994). Compared with other pathways of $Ca^{2+}$ entry in the neurons, what

would the role of the nAChR be? Unlike the NMDA and voltage-gated $Ca^{2+}$ channels, the nAChR channel conducts linearly at membrane potentials more negative than about −20 mV, where the $Ca^{2+}$ electrochemical gradient is stronger. The apparent specialization in operating at negative potentials is even more evident in the fact that the nAChR channel rectifies, being unable to allow $Ca^{2+}$ entry at depolarized potentials. This inward rectification was recently found to depend upon intracellular $Mg^{2+}$ (Alkondon et al., 1994), being much less prominent in fluoride-containing intracellular solutions (like the ones used here) because of the removal of $Mg^{2+}$ by $MgF_2$ precipitation (c.f. Zorumski et al., 1992; Zhang et al., 1994). Thus, α-BGT-sensitive nAChR channels provide a specific pathway for fast, $Ca^{2+}$-mediated transmembrane signaling at resting or hyperpolarized membrane potentials.

Because of a tight kinetic coupling between activation and desensitization, the true time course of the $Ca^{2+}$ signal conveyed by the nAChR channels is likely to be strongly dependent upon the dynamics of the agonist concentration. Two scenarios illustrate the different conditions under which the channels may operate in situ. First, consider the case of postsynaptic nAChR channels in a cholinergic synapse, as might occur in the rat hippocampus (Hunt and Schmidt, 1978). There, the transmitter would be present transiently in high concentration, being then quickly removed by diffusion and enzymatic hydrolysis. Synaptic activity would cause a fast $Ca^{2+}$ influx, both through the nAChR channels and, if the currents density suffices to depolarize the membrane, through voltage-dependent $Ca^{2+}$ channels. Desensitization would preclude immediate reactivation of the receptors and summation of currents, imparting a phasic characteristic on the transmission. Yet, the evidence for such an α-BGT-sensitive, nicotinic excitatory postsynaptic potential is lacking. A different situation arises in the case of extrasynaptic nAChRs. ACh released by a nearby cholinergic terminal would probably reach the receptor sites in lower and more slowly changing concentrations. Because the nAChR resensitization is fast, the asynchronous re-binding of ACh would generate long-lasting activity in the nAChR channel population, causing slow fluctuations in the intracellular $Ca^{2+}$ levels. In both situations, the control of $Ca^{2+}$ influx may be a mechanism by which ACh and α-BGT-sensitive nAChRs affect neuronal plasticity (Freeman, 1977; Vijayaraghavan et al., 1992). Accordingly, α-BGT-sensitive nAChRs were found to modulate neurite extension in PC12 (Chan and Quik, 1993) and chick ciliary ganglion cells (Pugh and Berg, 1994).

A final consideration is the interaction between the neuronal nAChRs and other neurotransmitter receptors. Muscarinic receptor activation causes excitation of hippocampal neurons by blocking several $K^+$ conductances (Storm, 1990), including $Ca^{2+}$-dependent components (Müller and Connor, 1991). If the cholinergic receptors were co-localized, the increase in membrane resistance due to muscarinic receptors could enhance the depolarization induced by activation of nearby α-BGT-sensitive nAChRs, as it does in the case of glutamate receptors (Müller and Connor, 1991). Also, if glutamatergic and cholinergic synapses occurred in close proximity, the nAChR-mediated $Ca^{2+}$ influx could directly affect the plasticity of the glutamatergic synapse (Malenka et al., 1988). Thus, besides having a well documented muscarinic component (e.g., Blitzer et al., 1990; Burgard and Sarvey, 1990), the cholinergic modulation of synaptic transmission in the hippocampus may involve α-BGT-sensitive nAChRs.

We are indebted to our colleagues in the laboratory, especially Dr. M. Alkondon and Ms. E. F. R. Pereira for comments on the manuscript, and Mrs. B. Marrow and Ms. M. Zelle for excellent technical assistance.
Support was provided by U.S. Public Health Service Grants NS25296 and ES05730, and a fellowship to N. G. Castro from CNPq, Brasília, Brazil.

## REFERENCES

Adams, D. J., T. M. Dwyer, and B. Hille. 1980. The permeability of endplate channels to monovalent and divalent metal cations. *J. Gen. Physiol.* 75: 493–510.

Adams, D. J., and T. J. Nutter. 1992. Calcium permeability and modulation of nicotinic acetylcholine receptor-channels in rat parasympathetic neurons. *J. Physiol. (Paris).* 86:67–76.

Alkondon, M., and E. X. Albuquerque. 1991. Initial characterization of the nicotinic acetylcholine receptors in rat hippocampal neurons. *J. Receptor Res.* 11:1001–1021.

Alkondon, M., and E. X. Albuquerque. 1993. Diversity of nicotinic acetylcholine receptors in rat hippocampal neurons. I. Pharmacological and functional evidence of distinct structural subtypes. *J. Pharmacol. Exp. Ther.* 265:1455–1473.

Alkondon, M., E. F. R. Pereira, S. Wonnacott, and E. X. Albuquerque. 1992. Blockade of nicotinic currents in hippocampal neurons defines methyllycaconitine as a potent and specific receptor antagonist. *Mol. Pharmacol.* 41:802–808.

Alkondon, M., S. Reinhardt, C. Lobron, B. Hermsen, A. Maelicke, and E. X. Albuquerque. 1994. Diversity of nicotinic acetylcholine receptors in rat hippocampal neurons. II. Rundown and inward rectification of agonist-elicited whole-cell currents and identification of receptor subunits by in situ hybridization. *J. Pharmacol. Exp. Ther.* 271:494–506.

Ascher, P., and L. Nowak. 1988. The role of divalent cations in the *N*-methyl-D-aspartate responses of mouse central neurones in culture. *J. Physiol.* 399:247–266.

Bertrand, D., J.-L. Galzi, A. Devillers-Thiéry, S. Bertrand, and J.-P. Changeux. 1993. Mutations at two distinct sites within the channel domain M2 alter calcium permeability of neuronal α7 nicotinic receptor. *Proc. Natl. Acad. Sci. USA.* 90:6971–6975.

Blitzer, R. D., O. Gil, and E. M. Landau. 1990. Cholinergic stimulation enhances long-term potentiation in the CA1 region or rat hippocampus. *Neurosci. Lett.* 119:207–210.

Burgard, E. C., and J. M. Sarvey. 1990. Muscarinic receptor activation facilitates the induction of long-term potentiation (LTP) in the rat dentate gyrus. *Neurosci. Lett.* 116:34–39.

Butler, J. N. 1968. The thermodynamic activity of calcium ion in sodium chloride-calcium chloride electrolytes. *Biophys. J.* 8:1426–1433.

Castro, N. G., and E. X. Albuquerque. 1993. Brief-lifetime, fast-inactivating ion channels account for the α-bungarotoxin-sensitive nicotinic response in hippocampal neurons. *Neurosci. Lett.* 164:137–140.

Castro, N. G., and E. X. Albuquerque. 1994. Calcium permeability of α-bungarotoxin-sensitive nicotinic acetylcholine receptors in rat hippocampal neurons. *Biophys. J.* 66:214*a*. (Abstr.)

Castro, N. G., A. T. Eldefrawi, and E. X. Albuquerque. 1993. Fast kinetics and calcium permeability of α-bungarotoxin-sensitive hippocampal nicotinic receptor channels. *Soc. Neurosci. Abs.* 19:464*a*. (Abstr.)

Chan, J., and M. Quik. 1993. A role for the nicotinic α-bungarotoxin receptor in neurite outgrowth in PC12 cells. *Neuroscience.* 56: 441–451.

Couturier, S., D. Bertrand, J.-M. Matter, M.-C. Hernandez, S. Bertrand, N. Millar, S. Valera, T. Barkas, and M. Ballivet. 1990. A neuronal nicotinic acetylcholine receptor subunit ($\alpha$7) is developmentally regulated and forms a homo-oligomeric channel blocked by $\alpha$-BTX. *Neuron.* 5:847–856.

Fieber, L. A., and D. J. Adams. 1991. Acetylcholine-evoked currents in cultured neurones dissociated from rat parasympathetic cardiac ganglia. *J. Physiol.* 434:215–237.

Freeman, J. A. 1977. Possible regulatory function of acetylcholine receptor in maintenance of retinotectal synapses. *Nature.* 269:218–222.

Goldman, D. E. 1943. Potential, impedance, and rectification in membranes. *J. Gen. Physiol.* 27:37–60.

Green, W. N., and O. S. Andersen. 1991. Surface charges and ion channel function. *Annu. Rev. Physiol.* 53:341–359.

Hamill, O. P., A. Marty, E. Neher, B. Sakmann, and F. J. Sigworth. 1981. Improved patch-clamp techniques for high resolution current recordings from cells and cell-free membrane patches. *Pflügers Arch.* 391:85–100.

Hirano, T., Y. Kidokoro, and H. Ohmori. 1987. Acetylcholine dose-response relation and the effect of cesium ions in the rat adrenal chromaffin cell under voltage clamp. *Pflügers Arch.* 408:401–407.

Hodgkin, A. L., and B. Katz. 1949. The effect of sodium ions on the electrical activity of the giant axon of the squid. *J. Physiol.* 108:37–77.

Hunt, S. P., and J. Schmidt. 1978. The electron microscopic autoradiographic localization of $\alpha$-bungarotoxin binding sites within the central nervous system of the rat. *Brain Res.* 142:152–159.

Iino, M., S. Osawa, and K. Tsuzuki. 1990. Permeation of calcium through excitatory amino acid receptor channels in cultured rat hippocampal neurones. *J. Physiol.* 424:151–165.

Ishihara, K., M. Alkondon, J. G. Montes, and E. X. Albuquerque. 1994. Nicotinic currents in neurons acutely dissociated from rat hippocampus and inhibition of the currents. *Soc. Neurosci. Abs.* 19:1138. (Abstr.)

Lewis, C. A. 1979. Ion-concentration dependence of the reversal potential and the single channel conductance of ion channels at the neuromuscular junction. *J. Physiol.* 286:417–445.

MacDonald, J. F., I. Mody, and M. W. Salter. 1989. Regulation of *N*-methyl-D-aspartate receptors revealed by intracellular dialysis of murine neurons in culture. *J. Physiol.* 414:17–34.

Malenka, R. C., J. A. Kauer, R. S. Zucker, and R. A. Nicoll. 1988. Postsynaptic calcium is sufficient for potentiation of hippocampal synaptic transmission. *Science.* 242:81–84.

Mathie, A., S. G. Cull-Candy, and D. Colquhoun. 1991. Conductance and kinetic properties of single nicotinic acetylcholine receptor channels in rat sympathetic neurones. *J. Physiol.* 439:717–750.

Mayer, M. L., and G. L. Westbrook. 1987. Permeation and block of N-methyl-D-aspartic acid receptor channels by divalent cations in mouse cultured central neurones. *J. Physiol.* 394:501–527.

Mulle, C., C. Lena, and J.-P. Changeux. 1992. Potentiation of nicotinic receptor response by external calcium in central neurons. *Neuron.* 8: 937–945.

Müller, W., and J. A. Connor. 1991. Cholinergic input uncouples $Ca^{2+}$ changes from $K^+$ conductance activation and amplifies intradendritic Ca2+ changes in hippocampal neurons. *Neuron.* 6:901–905.

Neuhaus, R., and A. B. Cachelin. 1990. Changes in the conductance of the neuronal nicotinic acetylcholine receptor channel induced by magnesium. *Proc. R. Soc. Lond. B.* 241:78–84.

Ochoa, E. L. M., A. Chattopadhyay, and M. G. McNamee. 1989. Desensitization of the nicotinic acetylcholine receptor: molecular mechanisms and effect of modulators. *Cell. Mol. Neurobiol.* 6:141–178.

Pugh, C. P., and D. K. Berg. 1994. Neuronal acetylcholine receptors that bind $\alpha$-bungarotoxin mediate neurite retraction in a calcium-dependent manner. *J. Neurosci.* 14:889–896.

Sands, S. B., and M. E. Barish. 1991. Calcium permeability of neuronal nicotinic acetylcholine receptor channels in PC12 cells. *Brain Res.* 560: 38–42.

Sands, S. B., A. C. S. Costa, and J. W. Patrick. 1993. Barium permeability of neuronal nicotinic receptor $\alpha$7 expressed in *Xenopus* oocytes. *Biophys. J.* 65:2614–2621.

Sargent, P. B. 1993. The diversity of neuronal nicotinic acetylcholine receptors. *Annu. Rev. Neurosci.* 16:403–443.

Schoepfer, R., W. G. Conroy, P. Whiting, M. Gore, and J. Lindstrom. 1990. Brain alpha-bungarotoxin binding protein cDNAs and MAbs reveal subtypes of this branch of the ligand-gated ion channel gene superfamily. *Neuron.* 5:35–48.

Robinson, R. A., and R. H. Stokes. 1970. Electrolyte Solutions. Butterworth, London.

Séguéla, P., J. Wadiche, K. Dineley-Miller, J. A. Dani, and J. W. Patrick. 1993. Molecular cloning, functional properties and distribution of rat brain $\alpha$7: a nicotinic cationic channel highly permeable to calcium. *J. Neurosci.* 13:596–604.

Storm, J. F. 1990. Potassium currents in hippocampal pyramidal cells. *Prog. Brain Res.* 83:161–187.

Vernino, S., M. Amador, C. W. Luetje, J. W. Patrick, and J. A. Dani. 1992. Calcium modulation and high calcium permeability of neuronal nicotinic acetylcholine receptors. *Neuron.* 8:127–134.

Vijayaraghavan, S., C. P. Pugh, Z.-W. Zhang, M. M. Rathouz, and D. K. Berg. 1992. Nicotinic receptors that bind $\alpha$-bungarotoxin on neurons raise intracellular free $Ca^{2+}$. *Neuron.* 8:353–362.

Zarei, M. M., and J. A. Dani. 1994. Ionic permeability characteristics of the N-methyl-D-aspartate receptor channel. *J. Gen. Physiol.* 103:231–248.

Zhang, Z.-W., S. Vijayaraghavan, and D. K. Berg. 1994. Neuronal acetylcholine receptors that bind $\alpha$-bungarotoxin with high affinity function as ligand-gated ion channels. *Neuron.* 12:167–177.

Zhou, Z., and E. Neher. 1993. Calcium permeability of nicotinic acetylcholine receptors in bovine adrenal chromaffin cells. *Pflügers Arch.* 425: 511–517.

Zorumski, C. F., L. L. Thio, K. E. Isenberg, and D. B. Clifford. 1992. Nicotinic acetylcholine currents in cultured postnatal rat hippocampal neurons. *Mol. Pharmacol.* 41:931–936.